Facile Synthesis and Visualization of Janus Double-Brush Copolymers

ARTICLE *in* ACS MACRO LETTERS · NOVEMBER 2011

Impact Factor: 5.76 · DOI: 10.1021/mz200013e

ACS Macro Letters

Letter

pubs.acs.org/macroletters

Facile Synthesis and Visualization of Janus Double-Brush Copolymers

Yukun Li, Efrosyni Themistou, Jiong Zou, Biswa P. Das, Marina Tsianou, and Chong Cheng*

Department of Chemical and Biological Engineering, University at Buffalo, The State University of New York, Buffalo, New York 14260, United States

Supporting Information

ABSTRACT: Well-defined double-brush copolymers with each graft site carrying a polystyrene (PSt) graft and a polylactide (PLA) graft were synthesized by simultaneous reversible addition−fragmentation chain transfer (RAFT) and ring-opening polymerization (ROP) processes, followed by ring-opening metathesis polymerization (ROMP) "grafting through" of the resulting diblock macromonomer (MM). Their Janus-type morphologies were detected by transmission electron microscopy (TEM) imaging after thermal annealing to facilitate the intramolecular self-assembly of PSt and PLA grafts. This finding provides critical evidence to verify double-brush copolymers as Janus nanomaterials.

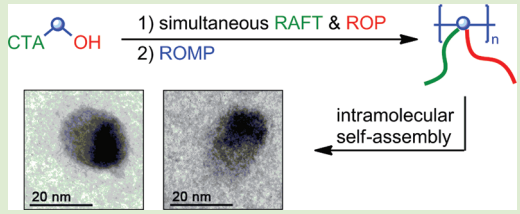

Since de Gennes highlighted the concept of "Janus grains" in his Nobel lecture in 1991,[1] Janus polymeric nanomaterials have attracted a broad interest.[2,3] With two chemically distinct domains that do not enclose each other, they may possess unique physical properties and potential applications in interfacial stabilization,[4,5] optical probes,[6] and the fabrication of Langmuir−Blodgett films or hierarchical superstructures.[7−11] Compared with aggregated non-centrosymmetric nanomaterials,[12−17] Janus unimolecular nanomaterials may possess enhanced structural stability and applicability. Elegant chemistries have been developed to achieve Janus unimolecular nanomaterials. A variety of Janus macromolecules with two different covalently linked nanostructured units or blocks have been reported.[18−21] For instance, Fréchet and co-workers have synthesized dendronized block copolymers with non-centrosymmetric morphologies.[20] The covalent stabilization of Janus micelles is also an important approach for the synthesis of Janus unimolecular nanomaterials. As demonstrated by Müller and co-workers, non-centrosymmetric nanoscopic particles, cylinders, and disks have been prepared from Janus micelles of triblock copolymers by selective cross-linking of the short middle blocks.[22−24] Moreover, Janus unimolecular nanoparticles can also be prepared by polymerization or modification in the presence of asymmetrical templates.[25,26] However, it remains a challenge to develop facile and scalable approaches for the preparation of unimolecular Janus nanomaterials and to verify their non-centrosymmetric nanostructures by visualization techniques.

Brush polymers (BPs) have emerged as an important class of nanostructured polymers.[27,28] Over the past decade, BPs with two statistically distributed types of immiscible grafts have received significant attention.[29−41] Typically, they were prepared by "grafting through",[29−33] "grafting from",[34,35] "grafting onto",[36] or combinations of these approaches,[37−40] requiring three sequential polymerization steps from small molecules. It has been broadly speculated that BPs may exhibit Janus conformation by intermolecular self-assembly of their heterografts. Such a speculation has been supported by the experimental studies on their surface morphology,[31] aggregation behavior, and interfacial properties,[32] as well as computational simulations.[41] However, to our best knowledge, visualization of the Janus conformation of heterografted BPs has not been reported. We ascribe this to two reasons. First, most of the heterografted BPs that have been reported do not possess well-defined grafting architectures with balanced numbers of heterografts on backbone segments. With unbalanced grafting, the intramolecular self-assembly of heterografts would lead to distorted phase-segregated morphologies, instead of well-defined Janus morphologies.[41] Second, the visualization of heterografted BPs was often conducted on surfaces selectively adsorbing one type of grafts, and such conditions were not suitable for the formation of detectable Janus conformations on an $x-y$ plane. As a type of model BPs, double-brush copolymers (DBCs) have each graft junction carrying two different grafts and, therefore, have identical distributions of heterografts along backbones.[42] As compared with other types of heterografted BPs, the structural features of DBCs may facilitate the formation of well-defined Janus conformations, which may be visualized under optimal conditions. Here, we describe our recent research on the facile synthesis and visualization of Janus conformation of DBCs.

A thoughtful design was made for the facile synthesis of DBCs with well-controlled structures (Scheme 1). Because quantitative grafting may not be guaranteed by "grafting from" and "grafting onto" approaches, a synthetic route of "grafting through" was selected. Instead of a mixture of two types of macromonomers (MMs),[29−33] a diblock MM with a pendent

Received: August 11, 2011
Accepted: September 12, 2011
Published: November 14, 2011

Scheme 1. Synthesis of DBCs 3, PNB−*g*−PSt/PLA

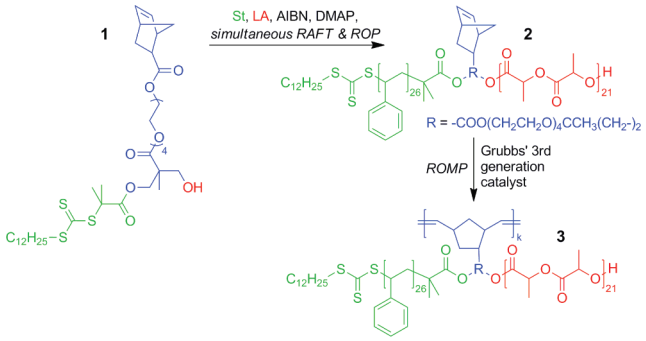

monomer functionality at the block junction was chosen for "grafting through" to ensure each graft site of the resulting BPs carrying two heterografts. Due to its high reactivity in ring-opening metathesis polymerization (ROMP), an *exo*-norbornene (NB) group was selected as the monomer functionality of the MM.[43] Serving as precursors of heterografts of DBCs, polystyrene (PSt) and polylactide (PLA) blocks were selected for the diblock MM because of their immiscibility.[34,44,45] Because of the compatibility of living radical polymerizations with ring-opening polymerization (ROP),[46−48] simultaneous reversible addition−fragmentation chain transfer (RAFT) polymerization of St and ROP of L-lactide (LA) were designed for the synthesis of the PSt−NB−PLA diblock MM.

The well-defined PSt−NB−PLA diblock MM was synthesized from small molecules by one-pot tandem polymerizations. A multifunctional agent **1** was prepared (see Figure S1a of the Supporting Information (SI)), and it has a trithiocarbonate chain transfer functionality for RAFT polymerization,[49] a hydroxyl group as an initiator site for ROP,[50,51] and an *exo*-NB functionality as the ROMP monomer group. By selecting azobisisobutyronitrile (AIBN) as the thermal initiator for RAFT polymerization of St and 4-dimethylaminopyridine (DMAP) as the organocatalyst for ROP of LA,[49,50] simultaneous polymerizations were conducted at 59 °C in the presence of **1** ($[\mathbf{1}]_0/[St]_0/[LA]_0/[AIBN]_0/[DMAP]_0$ = 1:70:35:0.1:4, 30 wt % of 1,2-dichloroethane). As detected by ^{1}H NMR spectroscopy, the occurrence of simultaneous polymerizations was verified by the continuous increase of conversions of both St and LA with polymerization time (Figure 1a). The polymerization was stopped at 24 h with 34% conversion of St and 71% conversion of LA, corresponding to the calculated number-average degree of polymerization (DP_n) of 24 for the PSt block and 25 for the PLA block of the resulting MM, that is, PSt−NB−PLA **2**. The well-defined macromolecular structure of **2** was verified by instrumental analysis. Because NB was stable under the conditions of RAFT polymerization and ROP,[51,52] DP_n for blocks of **2** can be determined by ^{1}H NMR analysis based on the comparison of the resonance intensities of aromatic protons of PSt at 6.28−7.60 ppm and the CH protons of PLA at 5.12−5.40 ppm with the resonance intensities of the NB alkene protons at 6.06−6.13 ppm (Figure 1b). The experimental DP_n of 23 for PSt block and 21 for PLA block were obtained, corresponding to the number-average molecular weight (M_n) of 6.2 kDa for **2**. These DP_n^{NMR} values were in good agreement with the calculated DP_n values, indicating well-controlled simultaneous polymerizations for the synthesis of **2**. Matrix-assisted laser desorption ionization time-of-flight (MALDI-TOF) analysis showed a narrow, monomodal molecular weight distribution of **2** with the peak molecular weight (M_p) of

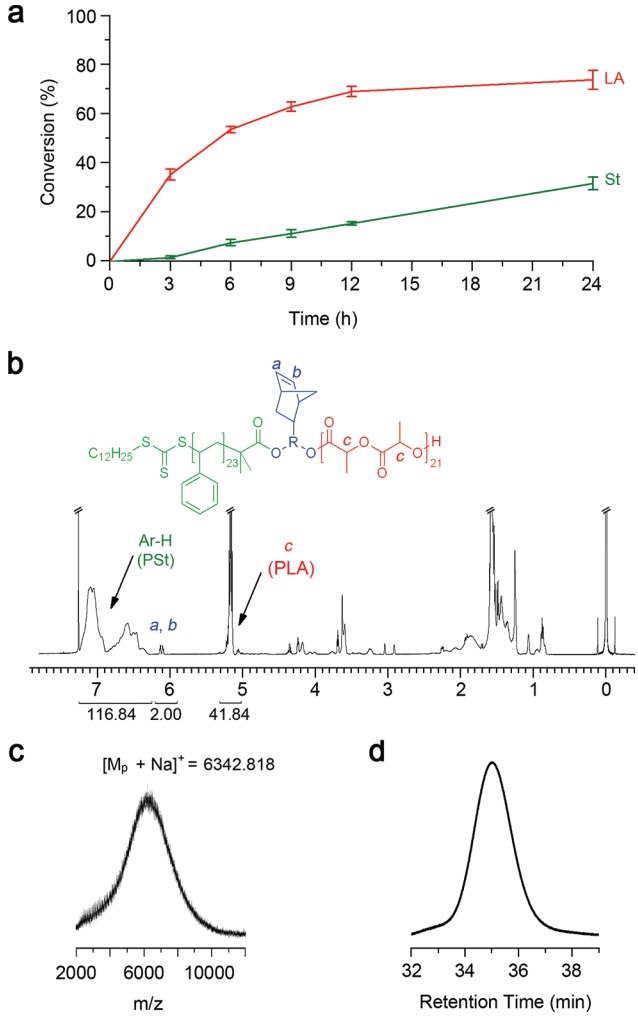

Figure 1. (a) Time dependence of conversions of St and LA for simultaneous RAFT and ROP processes in preparation of MM of PSt_{23}−NB−PLA_{21}, **2** (reaction conditions: $[\mathbf{1}]_0/[St]_0/[LA]_0/[AIBN]_0/[DMAP]_0$ = 1:70:35:0.1:4, 30 wt % of 1,2-dichloroethane, 59 °C); (b) ^{1}H NMR spectrum of **2**; (c) MALDI-TOF spectrum of **2**; (d) GPC curve of **2**.

6319.83 Da (Figure 1c), which was very close to the M_n^{NMR} of **2**. Gel permeation chromatography (GPC) analysis indicated that, relative to linear PSt, **2** had a M_n of 8.6 kDa and a narrow polydispersity index (PDI) of 1.14 (Figure 1d). Because the light scattering detector of the GPC instrument is not sensitive to polymer species with molecular weights less than about 5 kDa and diblock copolymers may differ with PSt standards in the relationship between MW and retention times, the M_n^{GPC} value of **2** might be overestimated.

Sequentially well-defined DBCs, that is, PNB−*g*−PSt_{23}/PLA_{21} **3**, were synthesized by ROMP of MM **2** (Table 1). The Grubbs' third generation catalyst was selected as the initiator for ROMP because of its high reactivity.[53−55] With different $[\mathbf{2}]_0$:$[Ru]_0$ values (59−176), polymerization experiments were conducted in CH_2Cl_2 at room temperature for 1 h. As determined by GPC analysis of polymerization solutions based on the peak areas of DBCs and the remaining MM, high conversions (86−95%) of **2** were obtained. Pure DBCs were obtained after passing the polymerization solutions through short columns of silica gel to trap unreacted **2** (Figure S2 of the SI).[56] The chemical structure of DBCs **3** was verified by ^{1}H

dx.doi.org/10.1021/mz200013e | *ACS Macro Lett.* 2012, 1, 52−56

Table 1. Synthesis of PNB−*g*−PSt$_{23}$/PLA$_{21}$ DBCs

entry	[**2**]$_0$/[Ru]$_0$	conv. %[a]	M_n (kDa) calcd[b]	M_n (kDa) GPC	PDI[c]	$D_{h,v}$[d] (nm)
3a	59:1	95	348	435	1.15	18.8
3b	117:1	91	660	748	1.24	24.0
3c	176:1	86	938	892	1.28	27.1

[a]Based on the RI signal from GPC analysis. [b]$M_n^{calcd} = ([\mathbf{2}]_0/[Ru]_0) \times M_{n,2}^{NMR} \times$ conv. % + 104. [c]By GPC with multiple detectors. [d]In CH_2Cl_2, by dynamic light scattering (DLS).

NMR analysis (Figure S1c of the SI). Well-defined structures of DBCs were verified by their narrow and monomodal GPC curves (Figure 2a; PDI = 1.15−1.28). On the basis of the

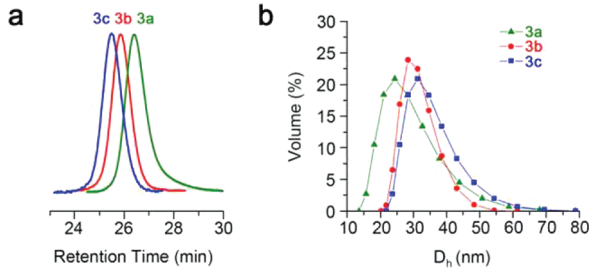

Figure 2. (a) GPC curves of PNB−*g*−PSt$_{23}$/PLA$_{21}$, DBCs **3**; (b) DLS size distribution profiles of DBCs **3** in CH_2Cl_2.

signals from both RI and light scattering detectors, the experimental M_n^{GPC} values of **3** measured by GPC were in good agreement with the calculated values, indicating the well-controlled ROMP processes. From the ratio of experimental $M_{n,3}/M_{n,2}$, DP$_n$ values of 70−143 can be estimated for the PNB-based backbones of these DBCs. Dynamic light scattering (DLS) measurements were conducted for DBCs **3** at room temperature in CH_2Cl_2, which is a good solvent for both PSt and PLA blocks (Figure 2b; Figure S3 of the SI). Reflecting the sizes of their unimolecular nanostructures in solution, volume-average hydrodynamic diameter ($D_{h,v}$) values ranging from 18.8 to 27.1 nm were obtained for **3**. These $D_{h,v}$ values increased with the M_n values of DBCs. Differential scanning calorimetry (DSC) measurement of DBC samples showed only one thermal transition temperature at 58.6 °C (Figure S4 of the SI), suggesting that self-assembly of PSt and PLA grafts could not occur considerably under the DSC measurement conditions to result in appreciable phase separation. According to thermogravimetric analysis (TGA), DBC samples exhibited an onset temperature of mass loss at around 231 °C, suggesting their stability below this characteristic temperature (Figure S5 of the SI). The significant thermal stability of these DBCs was further verified by their identical GPC curves before and after heating their dimethyl sulfoxide (DMSO) solutions at 180 °C for 12 h (Figure S6 of the SI).

Because **3c**, PNB$_{143}$−*g*−PSt$_{23}$/PLA$_{21}$, has the largest molecular size, it was selected as the representative DBC sample for visualization. Taping-mode atomic force microscopy (AFM) characterization was conducted to visualize the surface morphology of **3c** (Figure 3; Figure S7 of the SI). The AFM samples were prepared by spin-coating or solvent-casting of dilute CH_2Cl_2 solutions of **3c** on hydrophilic mica surfaces. With backbones much longer than heterografts, molecules of **3c** exhibited flattened cylindrical morphologies with an average length of 98 ± 14 nm, an average width of ~20 nm, and surface

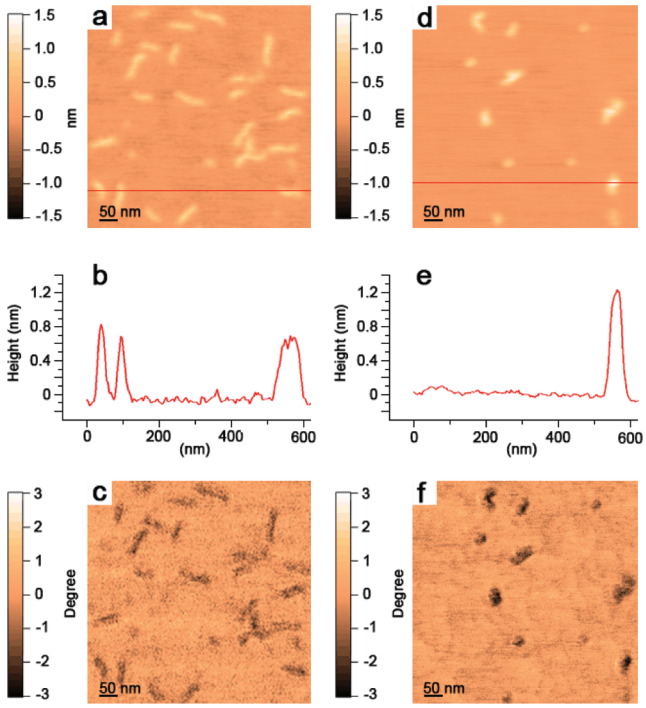

Figure 3. Tapping-mode AFM images of **3c** on mica: (a) height image, (b) height profile, and (c) phase image of the spin-coated sample; (d) height image, (e) height profile, and (f) phase image of the solvent-cast sample.

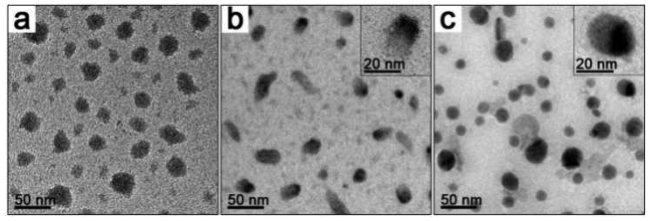

Figure 4. TEM images of **3c**: (a) without annealing, (b) after annealing at 150 °C for 12 h, and (c) after annealing at 180 °C for 12 h. The TEM samples were prepared by solvent-casting and stained by RuO_4.

height up to ~1.0 nm, because the centrifugal force during sample preparation forced them to take stretched conformations with extended backbones (Figure 3a−c). As a comparison, solvent-casting led to a decreased aspect ratio but increased surface height (up to 1.5 nm) for molecules of **3c** on mica surface, indicating their more contracted conformations (Figure 3d−f). Attempts were made to promote the self-assembly of the heterografts of **3c** by annealing the AFM samples at elevated temperatures (up to 180 °C for 12 h). However, well-defined phase segregation patterns of **3c** could not be observed by AFM phase imaging, presumably because the selective adsorption of hydrophilic PLA grafts by the hydrophilic mica surface led to phase segregation on the *z* dimension that cannot be readily detected by AFM.[34]

TEM imaging provided direct evidence for the presence of Janus conformations of the DBC (Figure 4). TEM samples were prepared by solvent-casting of dilute CH_2Cl_2 solutions of **3c** on carbon films of TEM grids. Relative to hydrophilic mica surface used in AFM characterization, the hydrophobic carbon substrate used in TEM measurement may induce smaller van der Waals force with samples, and therefore, would be less

dx.doi.org/10.1021/mz200013e | *ACS Macro Lett.* 2012, 1, 52−56

selective toward heterografts of **3c**. Before annealing, **3c** exhibited irregular particle-like morphologies with sizes of around 30 nm without appreciable phase segregation (Figure 4a), indicating no considerable occurrence of self-assembly of heterografts of the DBC during sample preparation. In principle, polymer self-assembly requires effective chain motions, which typically can be allowed at temperatures well above the glass transition temperature (T_g) for amorphous polymer blocks or above the melting temperature (T_m) for crystalline polymer blocks. Thus, thermal annealing was selected as the strategy to facilitate self-assembly of **3c**. Because the thermal transition temperatures for segregated PSt and PLA domains of **3c** could not be obtained by DSC measurement, the literature values of T_g of ~100 °C for PSt,[57] an amorphous polymer, and T_m of 173−178 °C for PLA,[58] a crystalline polymer, were considered. As a result, two TEM samples of **3c** were annealed at 150 and 180 °C, respectively, for 12 h to promote the self-assembly of **3c**. The annealing temperature of 150 °C may allow the chain motion in amorphous domains, but chain motion in the in situ formed PLA-rich crystalline domains would be prohibited; while the annealing temperature of 180 °C may permit chain motion of all grafts. After annealing at 150 °C for 12 h, **3c** demonstrated morphologies with increased aspect ratio and smoothed boundaries, and gradually changed darkness was observed within the nanoscopic domains for **3c** (Figure 4b; Figure S8a,b of the SI). The TEM results suggested the intermediate conformations of **3c**. Because the chain motion in PLA-rich crystalline domains was considerably restricted at 150 °C and PSt-rich amorphous domains had better mobility and lower density, the increased length of **3c** might be due to the flow of grafts of the PSt-rich domains. The "gradual-Janus" patterns, with PSt-rich and PLA-rich domains reflected by the darker and the lighter domains, respectively,[59] indicated that the occurrence of self-assembly of heterografts was significant but incomplete, and the interfaces of PSt-rich domains and PLA-rich domains were formed but did not reach minimal areas. On the other hand, after annealing at 180 °C for 12 h, round particles with an average surface diameter of 20.6 ± 5.8 nm were observed for **3c**; a minor portion of particles showed clearly Janus-type patterns with dark and light regions, while most particles showed the same level of darkness (Figure 4c; Figure S8c,d of the SI). Their round morphologies indicated that the fully allowed motions of grafts under the annealing conditions led to minimized surface areas for nanoscopic domains of **3c**. Reflecting the unimolecular dimensions of **3c**, the average surface diameter of these particles detected by TEM was smaller than the $D_{h,v}$ value of **3c** measured by DLS. Evolved from the intermediate conformations, two types of Janus conformations of DBC molecules with a complete self-assembly of heterografts and minimized interfacial areas can be further deduced. The particles showing evident non-centrosymmetric patterns possessed left−right Janus conformations on $x-y$ plane, with the PSt−PLA interfaces perpendicular to the carbon substrate. The particles exhibiting the same darkness within their nanoscopic domains were expected to take the up−down Janus conformations with the PSt−PLA interfaces parallel to the carbon substrate. The reason of the major presence of the second type of particles presumably was that the interfaces of PSt-rich domains and PLA-rich domains of intermediate conformations typically were close to parallel to the surface for flattened surface particles (Figure 5).

In summary, we have demonstrated the facile synthesis of DBCs and the microscopic imaging of their nanostructures.

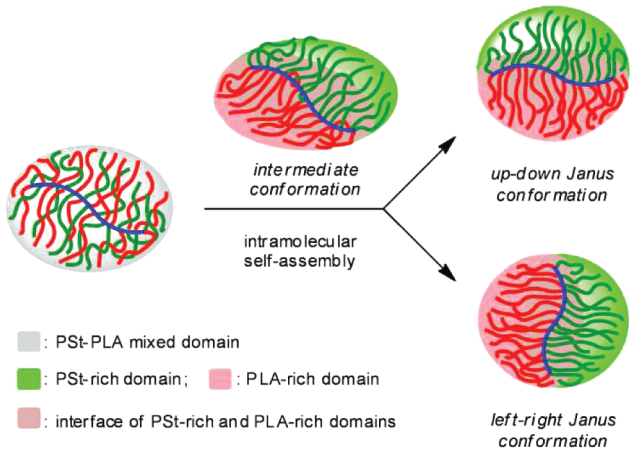

Figure 5. Schematic illustration of intramolecular self-assembly of DBCs.

Well-defined DBCs were synthesized by the preparation of PSt−NB−PLA by one-pot simultaneous RAFT polymerization and ROP, followed by "grafting through" of the diblock MM via ROMP. Such a simultaneous polymerization-based synthetic approach potentially may be employed to simplify the synthesis of other heterografted BPs. TEM and tapping mode AFM imaging of DBC molecules revealed their nanoscopic features. Particularly, the observation of their "gradual Janus" and left−right Janus conformations by TEM after annealing provided the direct experimental evidence to prove the DBCs as a type of Janus nanomaterial.

■ ASSOCIATED CONTENT

Supporting Information

Experimental details, ^{1}H NMR spectra of **1**, diblock MM and DBC **3c**, GPC curves of DBC **3c** before and after purification, DLS data of DBCs **3a−c**, DSC data of diblock MM and DBC **3c**, thermolytic profiles of diblock MM and DBC **3c**, GPC curves of DBC **3c** before and after heating, atomic force micrographs of DBC **3c** by spin-coating and by solvent-casting, and TEM images of DBC **3c** after annealing at 150 and 180 °C. This material is available free of charge via the Internet at http://pubs.acs.org.

■ AUTHOR INFORMATION

Corresponding Author

*E-mail: ccheng8@buffalo.edu.

Notes

The authors declare no competing financial interest.

■ ACKNOWLEDGMENTS

The authors thank Prof. Javid Rzayev and Dr. Yueling Qin for their kind assistance on characterization. This work was supported by startup funds from the University at Buffalo.

■ REFERENCES

(1) de Gennes, P. G. *Angew. Chem., Int. Ed.* **1992**, *31*, 842.
(2) Wurm, F.; Kilbinger, A. F. M. *Angew. Chem., Int. Ed.* **2009**, *48*, 8412.
(3) Jiang, S.; Chen, Q.; Tripathy, M.; Luijten, E.; Schweizer, K. S.; Granick, S. *Adv. Mater.* **2010**, *22*, 1060.
(4) Hawker, C. J.; Wooley, K. L.; Fréchet, J. M. J. *J. Chem. Soc., Perkins Trans. 1* **1993**, 1287.

(5) Walther, A.; Matussek, K.; Müller, A. H. E. *ACS Nano* **2008**, *2*, 1167.
(6) Behrend, C. J.; Anker, J. N.; Kopelman, R. *Appl. Phys. Lett.* **2004**, *84*, 154.
(7) Weber, E.; Akpo, C.; Reiche, U. *New J. Chem.* **2006**, *30*, 1820.
(8) Percec, V.; Wilson, D. A.; Leowanawat, P.; Wilson, C. J.; Hughes, A. D.; Kaucher, M. S.; Hammer, D. A.; Levine, D. H.; Kim, A. J.; Bates, F. S.; Davis, K. P.; Lodge, T. P.; Klein, M. L.; DeVane, R. H.; Aqad, E.; Rosen, B. M.; Argintaru, A. O.; Sienkowska, M. J.; Rissanen, K.; Nummelin, S.; Ropponen, J. *Science* **2010**, *328*, 1009.
(9) Walther, A.; Drechsler, M.; Rosenfeldt, S.; Harnau, L.; Ballauff, M.; Abetz, V.; Müller, A. H. E. *J. Am. Chem. Soc.* **2009**, *131*, 4720.
(10) Cheng, L.; Zhang, G. Z.; Zhu, L.; Chen, D. Y.; Jiang, M. *Angew. Chem., Int. Ed.* **2008**, *47*, 10171.
(11) Bo, Z.; Rabe, J. P.; Schlüter, A. D. *Angew. Chem., Int. Ed.* **1999**, *38*, 2370.
(12) Kietzke, T.; Neher, D.; Landfester, K.; Montenegro, R.; Güntner, R.; Scherf, U. *Nat. Mater.* **2003**, *2*, 408.
(13) Tanaka, T.; Nakatsuru, R.; Kagari, Y.; Saito, N.; Okubo, M. *Langmuir* **2008**, *24*, 12267.
(14) Higuchi, T.; Tajima, A.; Motoyoshi, K.; Yabu, H.; Shimomura, M. *Angew. Chem., Int. Ed.* **2008**, *47*, 8044.
(15) Xu, H.; Erhardt, R.; Abetz, V.; Müller, A. H. E.; Goedel, W. A. *Langmuir* **2001**, *17*, 6787.
(16) Voets, I. K.; de Keizer, A.; de Waard, P.; Frederik, P. M.; Bomans, P. H. H.; Schmalz, H.; Walther, A.; King, S. M.; Leermakers, F. A. M.; Cohen Stuart, M. A. *Angew. Chem., Int. Ed.* **2006**, *45*, 6673.
(17) Li, Z.; Hillmyer, M. A.; Lodge, T. P. *Langmuir* **2006**, *22*, 9409.
(18) Wooley, K. L.; Hawker, C. J.; Fréchet, J. M. J. *J. Am. Chem. Soc.* **1993**, *115*, 11496.
(19) Lanson, D.; Schappacher, M.; Borsali, R.; Deffieux, A. *Macromolecules* **2007**, *40*, 9503.
(20) Rajaram, S.; Choi, T. L.; Rolandi, M.; Fréchet, J. M. J. *J. Am. Chem. Soc.* **2007**, *129*, 9619.
(21) Feng, X.; Taton, D.; Ibarboure, E.; Chaikof, E. L.; Gnanou, Y. *J. Am. Chem. Soc.* **2008**, *130*, 11662.
(22) Erhardt, R.; Zhang, M. F.; Boker, A.; Zettl, H.; Abetz, C.; Frederik, P.; Krausch, G.; Abetz, V.; Müller, A. H. E. *J. Am. Chem. Soc.* **2003**, *125*, 3260.
(23) Liu, Y.; Abetz, V.; Müller, A. H. E. *Macromolecules* **2003**, *36*, 7894.
(24) Walther, A.; Andre, X.; Drechsler, M.; Abetz, V.; Müller, A. H. E. *J. Am. Chem. Soc.* **2007**, *129*, 6187.
(25) Zhang, S.; Li, Z.; Samarajeewa, S.; Sun, G.; Yang, C.; Wooley, K. L. *J. Am. Chem. Soc.* **2011**, *133*, 11046.
(26) Nie, L.; Liu, S.; Shen, W.; Chen, D.; Jiang, M. *Angew. Chem., Int. Ed.* **2007**, *46*, 6321.
(27) Sheiko, S. S.; Sumerlin, B. S.; Matyjaszewski, K. *Prog. Polym. Sci.* **2008**, *33*, 759.
(28) Zhang, M.; Müller, A. H. E. *J. Polym. Sci., Polym. Chem.* **2005**, *43*, 3461.
(29) Heroguez, V.; Gnanou, Y.; Fontanille, M. *Macromolecules* **1997**, *30*, 4791.
(30) Xia, Y.; Olsen, B. D.; Kornfield, J. A.; Grubbs, R. H. *J. Am. Chem. Soc.* **2009**, *131*, 18525.
(31) Stephan, T.; Muth, S.; Schmidt, M. *Macromolecules* **2002**, *35*, 9857.
(32) Ishizu, K.; Sawada, N.; Satoh, J.; Sogabe, A. *J. Mater. Sci. Lett.* **2003**, *22*, 1219.
(33) Zhang, Y.; Li, X.; Deng, G.; Chen, Y. *Macromol. Chem. Phys.* **2006**, *207*, 1394.
(34) Wu, D.; Yang, Y.; Cheng, X.; Liu, L.; Tian, J.; Zhao, H. *Macromolecules* **2006**, *39*, 7513.
(35) Xie, M.; Dang, J.; Han, H.; Wang, W.; Liu, J.; He, X.; Zhang, Y. *Macromolecules* **2008**, *41*, 9004.
(36) Fu, Q.; Liu, C.; Lin, W.; Huang, J. *J. Polym. Sci., Polym. Chem.* **2008**, *46*, 6770.
(37) Gu, L.; Shen, Z.; Zhang, S.; Lu, G.; Zhang, X.; Huang, X. *Macromolecules* **2007**, *40*, 4486.
(38) Yin, J.; Ge, Z.; Liu, H.; Liu, S. *J. Polym. Sci., Polym. Chem.* **2009**, *47*, 2608.
(39) Lian, X.; Wu, D.; Song, X.; Zhao, H. *Macromolecules* **2010**, *43*, 7434.
(40) Yuan, Y.-Y.; Du, Q.; Wang, Y.-C.; Wang, J. *Macromolecules* **2010**, *43*, 1739.
(41) Theodorakis, P. E.; Paul, W.; Binder, K. *Macromolecules* **2010**, *43*, 5137.
(42) Cheng, C.; Yang, N. L. *Macromolecules* **2010**, *43*, 3153.
(43) Maynard, H. D.; Okada, S. Y.; Grubbs, R. H. *Macromolecules* **2000**, *33*, 6239.
(44) Runge, M. B.; Dutta, S.; Bowden, N. B. *Macromolecules* **2006**, *39*, 498.
(45) Bolton, J.; Bailey, T. S.; Rzayev, J. *Nano Lett.* **2011**, *11*, 998.
(46) Le Hellaye, M.; Lefay, C.; Davis, T. P.; Stenzel, M. H.; Barner-Kowollik, C. *J. Polym. Sci., Polym. Chem.* **2008**, *46*, 3058.
(47) Thurecht, K. J.; Gregory, A. M.; Villarroya, S.; Zhou, J.; Heise, A.; Howdle, S. M. *Chem. Commun.* **2006**, 4383.
(48) Mecerreyes, D.; Moineau, G.; Dubois, P.; Jerome, R.; Hedrick, J. L.; Hawker, C. J.; Malmstrom, E. E.; Trollsas, M. *Angew. Chem., Int. Ed.* **1998**, *37*, 1274.
(49) Lai, J. T.; Filla, D.; Shea, R. *Macromolecules* **2002**, *35*, 6754.
(50) Nederberg, F.; Connor, E. F.; Moeller, M.; Glauser, T.; Hedrick, J. L. *Angew. Chem., Int. Ed.* **2001**, *40*, 2712.
(51) Jha, S.; Dutta, S.; Bowden, N. B. *Macromolecules* **2004**, *37*, 4365.
(52) Patton, D. L.; Advincula, R. C. *Macromolecules* **2006**, *39*, 8674.
(53) Li, Z.; Zhang, K.; Ma, J.; Cheng, C.; Wooley, K. L. *J. Polym. Sci., Polym. Chem.* **2009**, *47*, 5557.
(54) Johnson, J. A.; Lu, Y. Y.; Burts, A. O.; Lim, Y.-H.; Finn, M. G.; Koberstein, J. T.; Turro, N. J.; Tirrell, D. A.; Grubbs, R. H. *J. Am. Chem. Soc.* **2011**, *133*, 559.
(55) Zou, J.; Jafr, G.; Themistou, E.; Yap, Y.; Wintrob, Z. A. P.; Alexandridis, P.; Ceacareanu, A. C.; Cheng, C. *Chem. Commun.* **2011**, *47*, 4493.
(56) Cheng, C.; Khoshdel, E.; Wooley, K. L. *Nano Lett.* **2006**, *6*, 1741.
(57) *Polymer Handbook*, 4th ed.; Brandrup, J., Immergut, E. H., Grulke, E. A., Eds.; Wiley: New York, 1999.
(58) Middleton, J. C.; Tipton, A. J. *Biomaterials* **2000**, *21*, 2335.
(59) Trent, J. S.; Scheinbeim, J. I.; Couchman, P. R. *Macromolecules* **1983**, *16*, 589.